Magnetic Superlattices with Variable Interlayer Exchange Coupling: A New Approach for the Investigation of Low-Dimensional Magnetism

V. Leiner,[1,2,*] K. Westerholt,[1] A. M. Blixt,[3] H. Zabel,[1] and B. Hjörvarsson[3]

[1]*Institut für Experimentalphysik/Festkörperphysik, Ruhr-Universität Bochum, D-44780 Bochum, Germany*

[2]*LSS, Institut Laue-Langevin, F-38042 Grenoble Cedex, France*

[3]*Department of Physics, Uppsala University, Box 530, S-751 21 Uppsala, Sweden*

(Received 23 October 2002; published 15 July 2003)

We have investigated the magnetic order in an $[Fe_2/(VH_x)_{13}] \times 200$ superlattice as a function of temperature and hydrogen content in the vanadium layers. A $J_\perp$-T magnetic phase diagram was established where $J_\perp$ denotes the interlayer exchange coupling between adjacent Fe planes. We propose that Fe/V superlattices, in which the ratio of *interlayer* to *intralayer* coupling can be tuned continuously and reversibly via hydrogen in the nonmagnetic vanadium, offer a new approach for the study of low-dimensional magnetism and crossover effects near the transition from ferromagnetic to antiferromagnetic order.

DOI: 10.1103/PhysRevLett.91.037202 PACS numbers: 75.70.Ak, 75.30.–m, 75.40.Cx, 75.70.Cn

The interlayer exchange coupling (IEC) has been explored for many systems since it was first discovered in magnetic multilayers combining transition [1] or rare earth [2,3] metals and nonmagnetic [4] or semiconducting [5] interlayers. In various systems the IEC was found to be oscillatory, and both Ruderman-Kittel-Kasuya-Yosida- (RKKY-)like models [6,7] and a quantum interference model [8,9] predict oscillations of the interlayer exchange coupling $J_\perp$ with the Fermi wave vector k_F and the thickness of the nonmagnetic spacer layer, d_S, following $J_\perp \propto (2k_F d_S)^{-2} \sin(2k_F d_S)$. While the influence of d_S on the IEC has been widely studied, the influence of k_F is more difficult to test experimentally. Some examples exist, where the manipulation of the Fermi wave vector was achieved through alloying of the spacer layers [10–14]. Recently it was demonstrated for Fe/Nb [15,16] and Fe/V [17] superlattices that hydrogen incorporated in the nonmagnetic interlayers effectively changes k_F and thus the IEC.

In this Letter, we present an experimental investigation of the magnetic ordering in an $[Fe_2/(VH_x)_{13}] \times 200$ superlattice for hydrogen concentrations $x < 0.05$. The subscripts denote the number of monatomic layers and x is the hydrogen concentration defined as the atomic ratio, $x = \langle H/V \rangle$. We propose that the investigated system is highly relevant with respect to low-dimensional magnetism because of the strongly reduced thickness of the Fe films. Indeed the FM layers in the sample might be taken as two-dimensional magnets. Within the plane a ferromagnetic (FM) exchange coupling $J_\parallel$ arises from the direct exchange interaction between the Fe moments. The sign and strength of the out-of-plane IEC $J_\perp$ determine the three-dimensional (3D) magnetic structure of the sample. While the pristine Fe_2/V_{13} superlattice shows antiferromagnetic (AFM) order due to a negative $J_\perp$, at higher hydrogen concentrations $J_\perp$ becomes positive leading to a FM alignment of adjacent Fe layers [17]. Therefore, at a certain intermediate hydrogen concentration, the IEC should vanish and the decoupled Fe_2 layers display quasi-two-dimensional (2D) magnetic order. Earlier work on quasi-2D systems was based on the synthesis of layered ionic compounds [18]. Only very recently, with the investigation of Cr, $Nb/(Tb_{0.27}Dy_{0.73})_{0.32}Fe_{0.68}$ multilayers [19] and a Fe_2/V_5 superlattice [20], exchange coupled thin films have been used to address questions in low-dimensional magnetism. Here we use a new approach, namely, hydrogen in Fe/V(001) superlattices, and we report on the $J_\perp(x)$-T magnetic phase diagram of a $Fe_2/(VH_x)_{13}$ superlattice.

Two hundred repetitions of 2 monolayers (ML) of Fe and 13 ML of V were grown epitaxially by dc sputtering in a standard fashion [21] on an MgO(001) substrate (2×2 cm^2 in size). The sample quality and the thicknesses of the constituent layers were confirmed by x-ray characterization. Polarized and unpolarized neutrons were used to investigate the temperature and concentration dependences of the AFM order. The experiments were performed with the ADAM neutron reflectometer at the Institut Laue-Langevin, Grenoble [22]. A closed-cycle refrigerator (displex) was equipped with a closed container at the sample position and connected to an outside H-handling system. We loaded the sample by exposure to different pressures of hydrogen [23] at 300 K before cooling the sample to 10 K. During cooling, the hydrogen atmosphere was removed by evacuating the chamber at 250 K. When hydrogen enters the V layers an out-of-plane expansion of the V layers occurs and thus an increase of the superlattice period $\Lambda = d_{Fe} + d_{VH_x}$ is observed. This leads to a relative shift $\Delta Q/Q$ of the first-order superlattice peak to smaller values. From this shift we can determine the hydrogen concentration in the V layers via

$$\frac{\Delta d_V}{d_V} = k_S x, \tag{1}$$

with $k_S = 0.35$ and for $x \leq 0.1$ [25].

Complementary measurements were performed using a commercial SQUID (superconducting quantum interference device) magnetometer (Quantum Design MPMS). The SQUID setup does not allow an *in situ* exposure of the sample to a hydrogen atmosphere or a direct determination of x. Thus, the sample was loaded externally in a hydrogen atmosphere of 20 mbar, transferred to the SQUID, and quenched to 4 K for magnetization measurements. Some hydrogen was thereafter removed from the sample by heating to 400 K at 10 K/min in the He flow of the SQUID and cooling again at the same rate. After six such cycles the sample had returned to its initial state with all hydrogen removed. Comparing AFM transition temperatures determined by neutron reflectivity (NR) and the SQUID magnetization data (see below), we estimated that the H concentration during each thermal cycle decreases by about $\Delta x = 0.0075$.

Figure 1 shows NR curves taken with an unpolarized beam at 300 K (curve *A*) and 15 K (curve *C*). In curve *A*, a single peak is observed at $q = 0.270$ Å^{-1}, which corresponds to the chemical superlattice period Λ. Curve *B* shows a simulation obtained with values for the thicknesses of the various constituents of the superlattice determined from the x-ray characterization and literature values for the respective nuclear scattering length densities. In curve *C*, taken at 15 K, another peak is observed at a position that represents a modulation with a period of 2Λ. This peak arises from the AFM orientation of the magnetic moments in adjacent Fe layers [26–29]. Using a value of $0.37\mu_B$/Fe—obtained from SQUID magnetometry (see below)—for the absolute sublattice magnetization M, a simulation was performed (curve *D*), assuming perfect AFM order. We find that position, width, and amplitude of the simulated AFM peak are in excellent agreement with the experimental data, confirming that the complete magnetization contributes to the AFM order. Polarized neutron reflectometry measurements (inset in Fig. 1) further support the 180° coupling in the pristine sample, since no magnetic contribution to the intensity is observed at the first-order position.

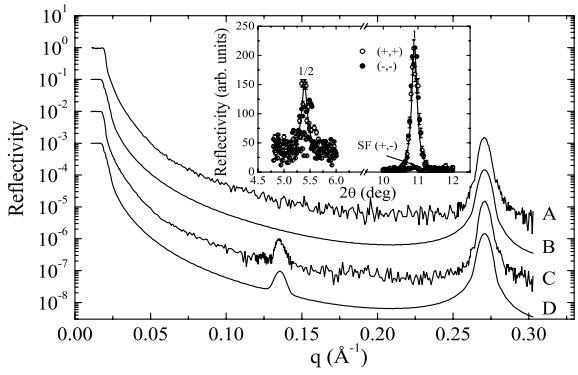

FIG. 1. Unpolarized NR curve of the pristine Fe_2/V_{13} superlattice taken above T_C (300 K) and at 15 K (curves *A* and *C*, respectively). Simulations (curves *B* and *D*) show that the complete magnetization contributes to the AFM order of the pristine sample. The inset shows data taken at 10 K with a polarized beam and employing spin analysis. No splitting is observed in the nonspin flip channels nor signal in the spin flip channel at the position of the first oder peak, supporting the notion of perfect AFM order in the pristine sample.

The AFM peak—its (integrated) intensity I is related to M via $I \propto |M|^2$—was investigated as a function of T with an unpolarized incident neutron beam. We obtained the magnetization curves, shown in Fig. 2, for the pristine sample and for two different hydrogen concentrations in the V layers. For the pristine superlattice, we find, in good agreement with the literature [30], a critical temperature $T_N \approx 92$ K. Upon dissolving hydrogen in the V layers, T_N decreases to 77 K for $|\Delta Q/Q| = 0.52\%$ and 67 K for $|\Delta Q/Q| = 0.63\%$, respectively. This represents a reduction of T_N by 30%. For $|\Delta Q/Q| = 0.83\%$, which was the next higher H concentration which we studied, the AFM peak is absent for all temperatures, showing that a transition to FM order has occurred. Using Eq. (1), we find that $|\Delta Q/Q| = 0.52\%$, $|\Delta Q/Q| = 0.63\%$, and $|\Delta Q/Q| = 0.83\%$ correspond to $x = 0.0173$, $x = 0.0206$, and $x = 0.0290$, respectively. Thus the introduction of very small amounts of hydrogen suffices to strongly affect the ordering temperature and eventually change the sign of the interlayer exchange interaction.

We now turn to the discussion of the SQUID magnetization study. Figure 3 shows typical magnetization curves measured at 5 K and with the external field applied in the sample plane. The magnetization curve for $x = 0$ is that of the pristine sample. The vanishing spontaneous magnetization confirms the perfect AFM state of the sample before exposure to hydrogen. Upon hydrogen exposure, initially, AFM order is maintained ($x = 0.0075$). However, a change in the shape of the magnetization curve is observed which arises from a reduced strength of $J_\perp$. The third curve ($x = 0.045$) depicts a typical FM magnetization curve with a large remanent magnetization. We measured magnetic hysteresis loops between 5 and 120 K in order to investigate the magnetic ordering as

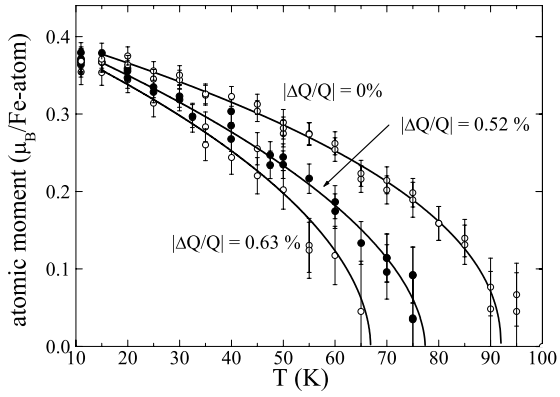

FIG. 2. Sublattice magnetization of the AFM coupled superlattice as a function of temperature for $|\Delta Q/Q| = 0, 0.52\%$ and 0.63%.

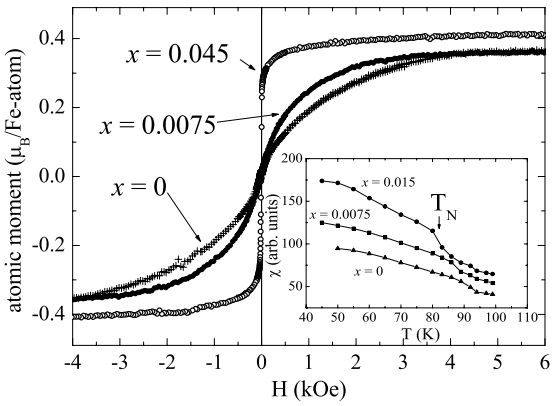

FIG. 3. In-plane magnetization curves for three different hydrogen contents at $T = 5$ K. Inset: susceptibility measurements in the AFM regime yield T_N at three different H concentrations. See the text for details.

a function of x. To determine T_C in the FM regime, we have plotted the squared remanent magnetization as a function of T and extrapolated towards vanishing remanence. The lowest observed value for T_C is 64 K at $x = 0.0225$; for higher concentrations T_C increases up to 93 K (see Table I). In the range of AFM order, at low x, we measured hysteresis loops between 4 and 100 K. In the inset in Fig. 3, we have plotted the susceptibility for the field-down cycle in an external field of 100 Oe. We determined the Néel temperature from a kink in the $\chi(T)$ curve which mainly originates from the onset of a small irreversibility near T_N. The Néel temperature shifts to higher values with decreasing hydrogen concentration and in state 7 reaches again the Néel temperature of the pristine state. Similarly, the AFM coupling field, defined as the external field necessary to ferromagnetically saturate the sample, coincides with that of the pristine sample state. Also SQUID magnetometry allows the determination of the absolute magnetic moment of the sample when a sufficiently high field is applied. Knowing the sample dimensions, we can evaluate absolute values for the magnetization M given in the μ_B/Fe atom. In Table I, we list the characteristics of the different sample states investigated in the SQUID study.

In Fig. 4(a), we have combined the magnetic ordering temperatures obtained from the neutron reflectivity study and SQUID results in a magnetic phase diagram (x-T diagram). The AFM-FM phase boundary is identified at a critical concentration $x_c \approx 0.022$. The transition temperature develops a deep minimum at this concentration with $T_{C,N}$ decreasing by about 30% from the FM and from the AFM side. In Fig. 4(b) we have plotted the AFM coupling field, i.e., $J_\perp$ in the AFM regime, as a function of x. We find a monotonic and approximately linear dependence of $J_\perp$ on x and the plot confirms that, as expected, hydrogen can be used to vary the IEC in an Fe/V superlattice. In the following we discuss the observed phase diagram in view of classical theoretical predictions. In the inset of Fig. 4(a) we reproduce a schematic phase diagram ($J_\perp$-T diagram [32]) presented by Griffiths [31] for an Ising model on a cubic lattice with a fixed, FM exchange $J_\parallel$ within one layer and a variable exchange $J_\perp$ between spins in adjacent layers. It is such a system that we endeavored to realize experimentally and indeed our phase diagram reproduces well the main features of the phase diagram predicted theoretically. For vanishing IEC, a crossover from 3D to 2D magnetic order should be expected, with a concomitant change of the critical exponents. Rüdt *et al.* [20] have recently shown for an $[Fe_2/V_5] \times 50$ superlattice that Fe_2 layers indeed display a 2D-Ising-like critical susceptibility exponent, $\gamma = 1.72(8)$, when $J_\perp$ vanishes [33].

In summary, we have shown that the magnetic phase diagram of an $[Fe_2/(VH_x)_{13}] \times 200$ superlattice exhibits a critical concentration $x_c \approx 0.022$ at which the magnetic order changes from AFM to FM. In the vicinity of x_c the transition temperature depends strongly on x and decreases continuously as x_c is approached. The intuitive concept that $J_\perp$ vanishes at x_c is supported by an investigation of the AFM coupling field as a function of x. The $J_\perp$-T phase diagram we present is in agreement with a theoretical, schematic phase diagram proposed for an Ising model on a cubic lattice with fixed intralayer and variable interlayer coupling. We propose that interlayer exchange coupled metallic superlattices in which the nonmagnetic spacer layers absorb hydrogen offer a

TABLE I. Parameters obtained from an analysis of the SQUID magnetization data for different hydrogen concentrations. In the SQUID experiments x and $|\Delta Q/Q|$ have been deduced indirectly. (See the text.)

State	Characterization	Magnetic order	$T_{C,N}$ (K)	$\lvert\Delta Q/Q\rvert$ (%)	x (%)	AFM coupling field (kOe)	M (μ_B/Fe atom)
1	Pristine	AFM	92	0	0	4.5(5)	0.37(1)
2	20 mbar H_2	FM	86	1.8	4.5	···	0.42(1)
3	2×400 K	FM	74	1.2	3.0	···	0.36(1)
4	3×400 K	FM	64	0.9	2.25	···	0.35(1)
5	4×400 K	AFM	82	0.6	1.5	2.5(3)	0.35(1)
6	5×400 K	AFM	88	0.3	0.75	2.8(4)	0.36(1)
7	6×400 K	AFM	93	0	0	4.3(5)	0.37(1)

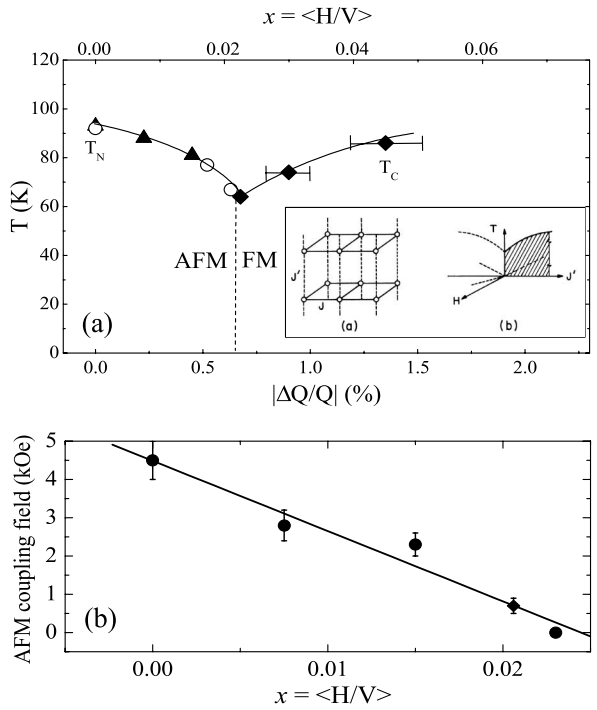

FIG. 4. (a) Magnetic phase diagram for an $[Fe_2/(VH_x)_{13}] \times 200$ superlattice determined by neutron reflectivity (open symbols) and SQUID (solid symbols). Lines are guides to the eye. Inset: phase diagram for a cubic Ising model with variable interlayer and fixed ferromagnetic intralayer coupling [31]. (b) Strength of the AFM coupling field as a function of x. The solid line is a linear fit to the data. The AFM coupling field at $x = 0.0206$ was determined by field-dependent NR.

new approach for studying systems in which magnetic order and dimensionality can be tuned continuously and reversibly.

This work was supported by the German Bundesministerium für Bildung und Forschung under Contract No. 04ZAE8BO. A. M. B and B. H. acknowledge support by the Swedish FRAM network and SSF.

*Electronic address: vincent.leiner@simeonics.com

[1] P. Grünberg, R. Schreiber, Y. Pang, M. B. Brodsky, and H. Sowers, Phys. Rev. Lett. **57**, 2442 (1986).
[2] M. B. Salamon, S. Sinha, J. J. Rhyne, J. E. Cunningham, R. W. Erwin, J. Borchers, and C. P. Flynn, Phys. Rev. Lett. **56**, 259 (1986).
[3] C. F. Majkrzak, J. W. Cable, J. Kwo, M. Hong, D. B. McWhan, Y. Yafet, J. V. Waszczak, and C. Vettier, Phys. Rev. Lett. **56**, 2700 (1986).
[4] D. E. Bürgler, P. Grünberg, S. O. Demokritov, and M. T. Johnson, in *Handbook of Magnetic Materials*, edited by K. H. J. Buschow (Elsevier North-Holland, Amsterdam, 2001), Vol. 13.
[5] M. Hunziker and M. Landolt, Phys. Rev. B **64**, 134421 (2001).
[6] S. Baltensperger and J. S. Helman, Appl. Phys. Lett. **57**, 2954 (1990).
[7] P. Bruno and C. Chappert, Phys. Rev. B **46**, 261 (1992).
[8] P. Bruno, Europhys. Lett. **23**, 615 (1993).
[9] A. Bounouh, P. Beauvillain, P. Bruno, C. Chappert, R. Mégy, and P. Veillet, Europhys. Lett. **33**, 315 (1996).
[10] S. S. P. Parkin, C. Chappert, and F. Herman, Europhys. Lett. **24**, 71 (1993).
[11] S. N. Okuno and K. Inomata, Phys. Rev. Lett. **70**, 1711 (1993).
[12] J.-F. Bobo, L. Hennet, M. Piecuch, and J. Hubsch, J. Phys. Condens. Matter **6**, 2689 (1994).
[13] M. van Schilfgaarde, F. Herman, S. S. P. Parkin, and J. Kudrnovský, Phys. Rev. Lett. **74**, 4063 (1995).
[14] Y. Endo, O. Kitakami, and Y. Shimada, Phys. Rev. B **59**, 4279 (1999).
[15] F. Klose, C. Rehm, D. Nagengast, H. Maletta, and A. Weidinger, Phys. Rev. Lett. **78**, 1150 (1997).
[16] P. H. Andersson, L. Fast, L. Nordström, B. Johansson, and O. Eriksson, Phys. Rev. B **58**, 5230 (1998).
[17] B. Hjörvarsson, J. A. Dura, P. Isberg, T. U. Watanabe, T. J. Udovic, G. Andersson, and C. F. Majkrzak, Phys. Rev. Lett. **79**, 901 (1997).
[18] *Magnetic Properties of Layered Transition Metal Compounds*, edited by L. J. de Jongh, Physics and Chemistry of Materials with Low-Dimensional Structures Vol. 9 (Kluwer Academic Publishers, Dordrecht, 1990).
[19] Ch. V. Mohan and H. Kronmüller, J. Magn. Magn. Mater. **182**, 287 (1998).
[20] C. Rüdt, P. Poulopoulos, J. Lindner, A. Scherz, H. Wende, K. Baberschke, P. Blomquist, and R. Wäppling, Phys. Rev. B **65**, 220404(R) (2002).
[21] P. Isberg, B. Hjörvarsson, R. Wäppling, E. B. Svedberg, and L. Hultman, Vacuum **48**, 483 (1997).
[22] www.ill.fr/YellowBook/ADAM
[23] For the neutron experiment the hydrogen isotope deuterium was used. For the V-H,D system strong isotope effects occur only at elevated concentrations $x \geq 0.35$ [24]. All our studies were performed in the low-concentration region, $x \leq 0.05$.
[24] Y. Fukai, *The Metal-Hydrogen System*, Springer Series in Materials Science Vol. 21 (Springer-Verlag, Heidelberg, 1993).
[25] G. Andersson, B. Hjörvarsson, and H. Zabel, Phys. Rev. B **55**, 15 905 (1997).
[26] S. J. Blundell and J. A. C. Bland, Phys. Rev. B **46**, 3391 (1992).
[27] G. P. Felcher, Physica (Amsterdam) **192B**, 137 (1993).
[28] H. Zabel, Physica (Amsterdam) **198B**, 156 (1994).
[29] G. P. Felcher and S. G. E. te Velthuis, Physica (Amsterdam) **297B**, 87 (2001).
[30] K. Eftimova, A. M. Blixt, B. Hjörvarsson, R. Laiho, and J. R. J. Salminen, J. Magn. Magn. Mater. **246**, 54 (2002).
[31] R. B. Griffiths, Phys. Rev. Lett. **24**, 1479 (1970).
[32] By some authors and in the inset in Fig. 4 J and J' are used instead of $J_{\|}$ and $J_{\perp}$, respectively.
[33] The vanishing of $J_{\perp}$ reported in Ref. [20] is argued to arise from the effect that $J_{\perp}$ decays faster than the magnetization as a function of T. Thus a decoupling occurs only near and above T_C (T_C^+) but not at low temperatures. We propose to "tune" $J_{\perp}$ to zero at all temperatures through the introduction of hydrogen.